

A HIGH-ORDER MATERIAL POINT METHOD

*Y. Ghaffari Motlagh¹ and W. M. Coombs¹

¹School of Engineering and Computing Sciences, Durham University
Science Site, South Road, Durham, DH1 3LE

*yousef.ghaffari-motlagh@durham.ac.uk

ABSTRACT

The material point method (MPM) is a version of the particle-in-cell (PIC) which has substantial advantages over pure Lagrangian or Eulerian methods in numerical simulations of problems involving large deformations. Using MPM helps to avoid mesh distortion and tangling problems related to Lagrangian methods and the advection errors associated with Eulerian methods. In this paper a novel high-order material point method within an isogeometric analysis (IGA) framework is developed. Utilizing high order basis functions enables more accurate determination of physical state variables e.g. stress. Smooth spline function spaces (B-splines) are used to eliminate the non-physical cell-crossing instabilities caused by use of standard finite element basis functions based on Lagrange polynomials.

Key Words: *material point method; implicit time integration; isogeometric analysis; B-splines*

1. Introduction

The material-point method (MPM) is a numerical method for solving continuum problems in fluid and solid mechanics. Its origins are the particle-in-cell (PIC) method developed at Los Alamos in the 1950s [1, 2] to model highly distorted fluid flow such as the splash of a falling drop. In the late 1980s, Brackbill and Ruppel [3] revived the PIC technology with simple modifications that reduced the numerical dissipation and made PIC competitive with current technologies for simulating hydrodynamics. The MPM [4, 5, 6] is a version of this method that is applicable to solids with strength and stiffness and has been applied to model diverse applications such as impact, penetration, fracture, metal forming, granular media and membranes.

In order to combine the advantages of Eulerian and Lagrangian methods, MPM uses two representations of the continuum. First, MPM discretises a continuum body of fluid or solid with a finite set of material points in the original configuration that are tracked throughout the deformation process. Each material point has a mass, position, velocity and stress, as well as material parameters and internal variables as needed for constitutive models or thermodynamics. These material points provide a Lagrangian description of the material that is not subject to mesh tangling because no connectivity is assumed between the points. The latter description, an Eulerian framework, is an often regular background mesh that covers the computational domain. Information is transferred from the material points to the background mesh, the momentum equation is solved on the background mesh, and then information from the mesh solution used to update the material points, at which time the background mesh can be modified if desired, the cycle then repeats.

Despite the MPM being promoted for its ability to solve large deformation problems it suffers from instabilities when material points cross between elements. These instabilities are due to the lack of smoothness of the grid basis functions used for mapping information between the material points and the background grid. By introducing a weighting function with higher degree of smoothness, the generalized interpolation material point (GIMP) method is capable of reducing these errors and improving accuracy [7]. Convected particle domain interpolation (CPDI) is another algorithm developed to improve the accuracy and efficiency of the material point method for problems involving extremely large tensile

deformation and rotation [8]. However, both methods require the basis functions (normally taken to be linear) to be integrated over the domain of the material point of interest, they also do not fully eliminate spurious oscillations due to cell crossing. In this paper an alternative approach is suggested where smooth B-spline function spaces are used to map between the material points and the background grid. The high-order smoothness of the splines eliminates the cell-crossing instability.

2. The quasi-static implicit material point method

Let us start by recalling the elastostatic equations. Let $\Omega \subset \mathbb{R}^d, d = 2, 3$, denote the domain occupied by the body, and let $\Gamma = \partial\Omega$ be its boundary. Then

$$\nabla \cdot \boldsymbol{\sigma} + \mathbf{f} = \mathbf{0} \quad \text{in } \Omega, \quad \mathbf{u} = \mathbf{g} \quad \text{on } \Gamma_D, \quad \text{and} \quad \boldsymbol{\sigma} \cdot \mathbf{n} = \mathbf{h} \quad \text{on } \Gamma_N, \quad (1)$$

where $\boldsymbol{\sigma}$ denotes the symmetric Cauchy stress tensor and \mathbf{f} is the body force per unit volume, \mathbf{u} is the displacement, \mathbf{g} and \mathbf{h} are referred as essential, Dirichlet, and natural, Neumann boundary condition, respectively. Here we restrict ourselves to small-strain analysis, where the small strain approximation, denoted by $\boldsymbol{\epsilon}$, is computed as the symmetric part of the displacement gradient $\boldsymbol{\epsilon} = (\nabla \mathbf{u} + (\nabla \mathbf{u})^T)/2$. The constitutive relationship, $\boldsymbol{\sigma} = \boldsymbol{\sigma}(\boldsymbol{\epsilon})$, is necessary to form a complete set of equations for computing the state variable, \mathbf{u} . Here we assume a linear isotropic relationship between strain and the Cauchy stress.

2.1. Discrete form

The continuum body Ω is discretised by finite set of N_p material points $\{\mathbf{x}_p\}_{p=1}^{N_p} \in \Omega$ in the original configuration that are tracked throughout the deformation process. Also, space is discretised by a background mesh defined by a set of N_n control points $\{\mathbf{x}_i\}_{i=1}^{N_n}$. The discrete MPM equilibrium equations are constructed by pre-multiplying the strong form of equilibrium (1) by a weighting function and applying integration by parts. A simple one-point quadrature rule is applied over each volume Ω_p associated with the p th material point to give

$$-\sum_{p=1}^{N_p} \{(\boldsymbol{\sigma}(\mathbf{x}_p) : \nabla \mathbf{w}^h(\mathbf{x}_p))\Omega_p\} + (\mathbf{h}, \mathbf{w}^h)_{\Gamma_N} + \sum_{p=1}^{N_p} \{(\mathbf{f}(\mathbf{x}_p) \cdot \mathbf{w}^h(\mathbf{x}_p))\Omega_p\} = \mathbf{0}. \quad (2)$$

(2) is solved on a finite dimensional space using functions represented in terms of B-spline basis functions, N_i^q . A B-spline basis is constructed from piece-wise polynomials joined with a prescribed continuity. In order to define a B-spline basis of polynomial order q in one dimension it is necessary to define a *knot vector*. A knot vector in one dimension is a set of coordinates in the parametric space, written as

$$\Xi = \{0 = \xi_1, \xi_2, \dots, \xi_{n+q+1} = 1\} \quad (3)$$

where $\xi_1 \leq \xi_2 \leq \dots \leq \xi_{n+q+1}$ and n is the total number of basis functions. Given Ξ and q , univariate B-spline basis functions are constructed recursively starting with piecewise

$$N_i^0(\xi) = \begin{cases} 1 & \text{if } \xi_i \leq \xi < \xi_{i+1} \\ 0 & \text{otherwise} \end{cases} \quad (4)$$

For $q = 1, 2, 3, \dots$, they are defined by

$$N_i^q(\xi) = \frac{\xi - \xi_i}{\xi_{i+q} - \xi_i} N_i^{q-1}(\xi) + \frac{\xi_{i+q+1} - \xi}{\xi_{i+q+1} - \xi_{i+1}} N_{i+1}^{q-1}(\xi) \quad (5)$$

Note that when $\xi_{i+q} - \xi_i = 0$, $(\xi - \xi_i)/(\xi_{i+q} - \xi_i)$ should be vanished, and similarly, when $\xi_{i+q+1} - \xi_{i+1} = 0$, $(\xi_{i+q+1} - \xi)/(\xi_{i+q+1} - \xi_{i+1})$ is taken to be zero as well. These basis functions have the following properties: (i) they form a partition of unity, (ii) have local support and (iii) are non-negative (for more details see [9]).

The explicit representation of $\mathbf{w}^h(\mathbf{x})$ in terms of the basis functions and control variables is assumed to take the standard form

$$\mathbf{w}^h(\mathbf{x}) = \sum_{i=1}^{N_n} N_i^q \mathbf{w}_i(\mathbf{x}). \quad (6)$$

Substituting the weighting function approximation into (2) and after simplification, the discrete MPM equation is obtained as

$$-\sum_{p=1}^{N_p} \{(\boldsymbol{\sigma}(\mathbf{x}_p) \cdot \nabla N_i^q(\mathbf{x}_p)) \Omega_p\} + \int_{\Gamma_N} \mathbf{h} N_i^q d\Gamma + \sum_{p=1}^{N_p} \{\mathbf{f}(\mathbf{x}_p) N_i^q(\mathbf{x}_p) \Omega_p\} = \mathbf{0}. \quad (7)$$

The numerical solution of this quasi-static problem is typically obtained in steps by incrementally imposing displacement boundary conditions, external forces or both in order to obtain increment in displacement, $\Delta \mathbf{u}$. Here a fully implicit method is employed to solve the problem. Once the displacement increment is obtained, the material point position, \mathbf{x}_p , and displacement, \mathbf{u}_p , are updated as follows

$$\mathbf{x}_p^{k+1} = \mathbf{x}_p^k + \sum_{i=1}^{N_n} \Delta \mathbf{u}_i N_i^q(\mathbf{x}_p^k) \quad \text{and} \quad \mathbf{u}_p^{k+1} = \mathbf{u}_p^k + \sum_{i=1}^{N_n} \Delta \mathbf{u}_i N_i^q(\mathbf{x}_p^k), \quad (8)$$

where k denotes the loadstep number. After each load step, the spatial position of background grid is reset to its original undeformed state.

3. Numerical results

Here we present the numerical results for a one-dimensional elastic column quasi-statically compressed by its own weight through the application of a body force, b_f , per unit mass. The initial material density $\rho_0 = 1$, Young's modulus $E = 10^6$, and initial column height $L_0 = 50$, all in compatible units. The column initially occupies 50 elements and the body force was applied over 20 loadsteps.

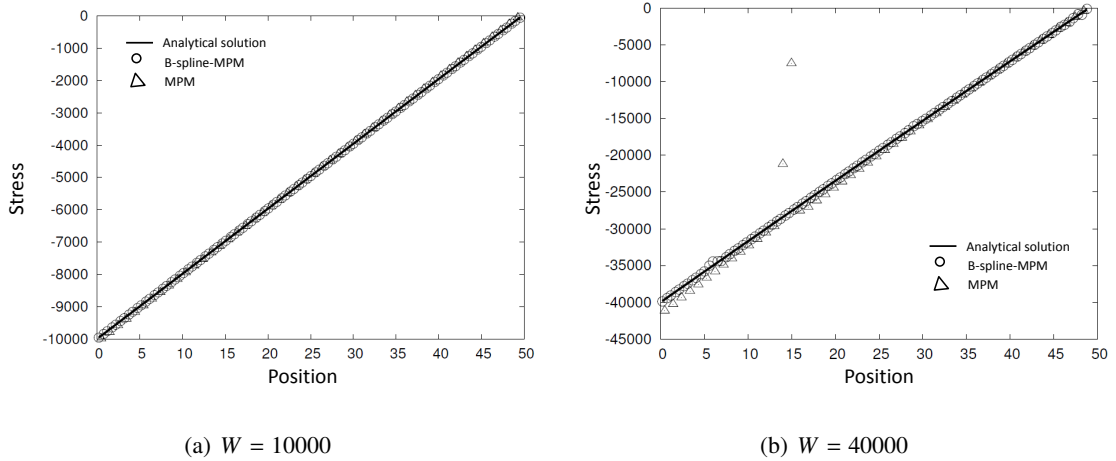


Figure 1: Numerical and analytical solutions to the one-dimensional elastic column quasi-statically compressed by its own weight under a body force

Figure 1 shows the stress distribution with $b_f = -200$ and $b_f = -800$, that is with a total column weight of $W = \rho_0 |b_f| L_0 = 10000$ and $W = 40000$, respectively. Results are shown for the standard MPM with linear basis functions and for the quadratic B-spline MPM ($q = 2$) and compared against the analytical solution (as provided in [7]). For the MPM the problem is initially discretised with one particle per grid cell as, for this very simple problem, increasing the number of material points reduces the accuracy of the simulation. The B-spline MPM used two particles per grid cell. In both cases the material points are initially located at the appropriate Gauss quadrature locations within the elements. When $b_f = -200$ both the methods provide a reasonable approximation to the analytical solution. However, for $b_f = -800$

spurious oscillations can be seen in the MPM results caused by cell-cross instabilities. These oscillations have been removed by the higher-order basis functions in the B-spline MPM.

Table 1 details the errors in the simulations based on the following error measure and the exact solution at the current particle locations [7]

$$\text{error} = \sum_{p=1}^{N_p} \frac{V_p |\sigma_p - \sigma_A(x_p)|}{WL_0}, \quad \text{where} \quad \sigma_A(x_p) = E \left(\sqrt{\frac{2\rho_0 b_f}{E} (L - x_p) + 1} - 1 \right) \quad (9)$$

and $L = L_0 + \rho_0 b_f L_0^2 / (2E)$ is the current length of the column. x_p is the particle location, V_p is the volume associated with the material point, σ_p is the material point stress. Errors have also been provided for an implicit GIMP implementation with two material points per original grid cell but have not been shown on Figure 1 for the sake of clarity.

total column weight, W	10,000	40,000
MPM	3.667×10^{-3}	2.572×10^{-2}
GIMP	3.680×10^{-3}	2.969×10^{-3}
B-spline MPM ($q = 2$)	6.221×10^{-5}	9.894×10^{-4}

Table 1: One-dimensional elastic column errors

It is clear from Table 1 that the B-spline MPM is an improvement over both the standard MPM and the GIMP method.

4. Conclusions

This paper has presented a MPM where the standard linear basis functions have been replaced by B-splines. The higher order smoothness of the splines significantly improves the accuracy of the method by removing the cell-cross instabilities seen in other MPMs.

Acknowledgements

The authors acknowledge the support of EPSRC grant EP/M017494/1.

References

- [1] F. Harlow. Hydrodynamics problems involving large fluid distortions, *J. Assoc. Compos. Mach.*, 4, 137, 1957.
- [2] M. Evans, F. Harlow. The particle-in-cell method for hydrodynamic calculations, *Tech. Rep. LA-2139, Los Alamos Sci. Lab., Los Alamos, N. M.*, 1957.
- [3] J. U. Brackbill, H. M. Ruppel. Flip: A method for adaptively zoned, particle-in-cell calculations in two dimensions, *J. Comput. Phys.*, 65, 314, 1986.
- [4] D. Sulsky, Z. Chen, H. L. Schreyer. A particle method for history-dependent materials, *Comput. Methods Appl. Mech. Eng.*, 118, 179-196, 1994.
- [5] D. Sulsky, S. J. Zhou, H. L. Schreyer. Application of a particle-in-cell method to solid mechanics, *Comput. Phys. Commun.*, 87, 236-252, 1995.
- [6] D. Sulsky, H. L. Schreyer. Axisymmetric form of the material point method with applications to upsetting and Taylor impact problems, *Comput. Methods Appl. Mech. Eng.*, 139, 409-429, 1996.
- [7] S. Bardenhagen, E. Kober. The generalized interpolation material point method, *CMES-Computer Modeling in Engineering and Sciences*, 5, 477-495. 2004.
- [8] A. Sadeghirad, R. M. Brannon, J. Burghardt. A convected particle domain interpolation technique to extend applicability of the material point method for problems involving massive deformations, *Int. J. Numer. Meth. Engng*, 86, 1435-1456, 2011.
- [9] L. Piegl, W. Tiller. *The NURBS Book (Monographs in Visual Communication)*, 2nd Edition., Springer-Verlag, New York, 1997.